

Continual Learning to Generalize Forwarding Strategies for Diverse Mobile Wireless Networks

Cheonjin Park Victoria Manfredi Xiaolan Zhang Chengyi Liu Alicia Wolfe
University of Connecticut Wesleyan University Fordham University Wesleyan University Wesleyan University
Storrs, CT, USA Middletown, CT, USA Bronx, NY, USA Middletown, CT, USA Middletown, CT, USA
cheon.park@uconn.edu vumanfredi@wesleyan.edu xzhang@fordham.edu tliu02@wesleyan.edu pwolfe@wesleyan.edu

Dongjin Song Sarah Tasneem Bing Wang
University of Connecticut Eastern Connecticut State University University of Connecticut
Storrs, CT, USA Willimantic, Connecticut, USA Storrs, CT, USA
dongjin.song@uconn.edu tasneems@easternct.edu bing@uconn.edu

Abstract—Deep reinforcement learning (DRL) has been successfully used to design forwarding strategies for multi-hop mobile wireless networks. While such strategies can be used directly for networks with varied connectivity and dynamic conditions, developing generalizable approaches that are effective on scenarios significantly different from the training environment remains largely unexplored. In this paper, we propose a framework to address the challenge of generalizability by (i) developing a generalizable base model considering diverse mobile network scenarios, and (ii) using the generalizable base model for new scenarios, and when needed, fine-tuning the base model using a small amount of data from the new scenarios. To support this framework, we first design new features to characterize network variation and feature quality, thereby improving the information used in DRL-based forwarding decisions. We then develop a continual learning (CL) approach able to train DRL models across diverse network scenarios without “catastrophic forgetting.” Using extensive evaluation, including real-world scenarios in two cities, we show that our approach is generalizable to unseen mobility scenarios. Compared to a state-of-the-art heuristic forwarding strategy, it leads to up to 78% reduction in delay, 24% improvement in delivery rate, and comparable or slightly higher number of forwards.

I. INTRODUCTION

Mobile wireless networks have been used for many applications, including emergency response, environmental monitoring, and military communications. Forwarding strategies for such networks aim to identify good paths over which to deliver data packets from source to destination. While many forwarding strategies have been developed, they typically target specific kinds of network connectivity. In ad hoc networks, for example, despite node movement, end-to-end paths often exist but only for short periods of time and so must be periodically updated [1]–[4]. In comparison, in delay-tolerant networks [5], contemporaneous end-to-end paths rarely exist and so packets must be forwarded hop-by-hop.

In reality, a mixture of good and bad connectivity may co-exist in a mobile wireless network, varying as a function of node movement [6]. Because network connectivity can change over time and space, it can be difficult for a node to ascertain whether a viable path exists to a packet’s destination

based on local neighborhood information; this then makes it difficult for the node to determine the right forwarding strategy. Deep reinforcement learning (DRL), which combines RL [7] with deep neural networks (DNNs) [8], is one approach to design forwarding strategies able to adapt to the changing network connectivity. With DRL, each node inputs a set of features characterizing its current state and possible next-hop actions into a DNN, which then generates outputs to inform forwarding decisions.

While DRL has been successfully used to design routing and forwarding strategies for a number of different network settings (see §II), the strategies are often tested in scenarios that are somewhat similar to the training environment. For instance, although the study in [9] develops DRL forwarding strategies across different network scenarios, including different transmission ranges and mobility models, its scope is limited to homogeneous networks. As such, the trained strategies are not suitable for use in highly diverse mobility scenarios.

An ideal generalizable forwarding strategy should function well in any mobile wireless network, including those it has never encountered in training. One way to achieve this generalization is through online training, i.e., retraining a model on the fly when encountering a new network scenario (see §II). Online training, however, takes time to converge, particularly in sparse networks where nodes have few opportunities to meet each other, and its performance tends to be poor before convergence. In addition, it can incur significant computational overhead, not suitable for devices with limited resources.

In this paper, we are particularly interested in forwarding strategies that are trained *offline*, where a model is trained beforehand and then used directly in a new scenario. This is a significant challenge, considering the potentially infinite number of possible mobile network scenarios. We propose a framework to address this challenge by first developing a *generalizable base model* trained on diverse mobile network scenarios. We then use this base model for *forwarding in new scenarios*; when needed, we *fine-tune* the base model using

only a small amount of data from a new scenario, and then use it for forwarding in similar scenarios. We identify two key components for developing a generalizable base model: (i) include a *rich set of features* to characterize network variation and feature quality, and (ii) use *continual learning (CL)* [10]–[12] to adapt to diverse network scenarios. Specifically, we make the following contributions:

- *Characterization of diverse mobile wireless networks (§IV)*. We propose three new classes of features to characterize network diversity: (i) quality-of-information metrics, (ii) network memory metrics, and (iii) community metrics. Features in these classes evaluate information about the network over time, and hence can provide valuable information even when instantaneous features have become out-of-date. We show that these features are important for characterizing heterogeneous network conditions, and for training a base forwarding model that is generalizable across diverse network scenarios.
- *Generalizable policy trained using CL (§V)*. We address the challenge of generalizing DRL-based forwarding strategies to disparate network scenarios through the use of CL. We design a simple and robust method that learns generalizable forwarding strategies using CL from multiple diverse network scenarios without suffering from “catastrophic forgetting”.
- *Extensive evaluation (§VI) and real-world scenarios (§VII)*. Using evaluation in 21 small and 36 large synthetic network scenarios, as well as 18 real-world scenarios in two cities that cover a wide range of network density, connectivity and mobility models, we show that our approach is generalizable. It outperforms a state-of-the-art heuristic strategy in most scenarios, achieving up to 78% reduction in delay, 24% improvement in delivery rate, and incurring comparable or slightly more forwards.

II. RELATED WORK

RL and DRL for routing. Q-routing [13] is the first scheme that uses RL [7] for routing. Since then, many more schemes that use RL or DRL have been proposed (see surveys [14]–[17]). Existing DRL-based routing and forwarding strategies for mobile wireless networks typically target specific network types, e.g., vehicular networks [18]–[20], UAV networks [21]–[24], IoT networks [25]. In addition, most studies focus on online learning (e.g., as in Q-routing [13]), which is much less efficient than offline training. The study most closely related to ours is [9], which, like our work, employs offline training. We nevertheless examine a significantly broader range of networks (including real road networks) than does [9], and focus on improving generalizability across diverse networks by proposing novel features and developing CL-based approaches.

CL. Many CL techniques have been developed that allow training of an intelligent system using new tasks without forgetting what was learned in earlier tasks [10]–[12]. We adopt a replay-based technique to our problem setting. While CL has been used in many applications, only a few studies explore its use in computer networks. The study in [26] uses CL to adapt routing to time-varying conditions (e.g., traffic,

link states, and mobility patterns) in Low Earth Orbit satellite networks. It employs CL in an online manner, whereas our study uses CL in an offline manner. Other studies use CL for other contexts, such as resource allocation [27].

Characterizing heterogeneous mobile networks. In this work we identify new classes of features to characterize heterogeneity in mobile networks. While some of the features that we propose for these classes have been identified in previous works (see [28]–[30] and §IV), they have not previously been used in a DRL context. We additionally design new features for these classes, particularly the short and long dispersion features in §IV-B. For all features, we design methods for easy online estimation in deployed mobile networks.

III. BACKGROUND AND HIGH-LEVEL APPROACH

In this section, we briefly overview DRL, and then present the main ideas in our DRL-based approach to generalize forwarding strategies across diverse mobile wireless networks.

A. DRL Background

In RL [7], an agent interacts with its environment to learn a policy, i.e., the best action for each state of the environment. A Markov decision process (MDP) is used to model this policy, defined as a 4-tuple $(\mathcal{S}, \mathcal{A}, \mathcal{P}, \mathcal{R})$ where \mathcal{S} is the set of states and $\mathcal{A}(s)$ are the actions available in each state $s \in \mathcal{S}$, while $\mathcal{P}(s, a, s')$ is a function giving the probability of transitioning from state $s \in \mathcal{S}$ to $s' \in \mathcal{S}$ after taking action $a \in \mathcal{A}$ and $\mathcal{R}(s, a, s')$ is a function giving the corresponding reward. In RL, \mathcal{P} and \mathcal{R} are not known, but samples can be obtained via interactions with the environment and used to learn a Q-value for each (s, a) pair, $s \in \mathcal{S}$ and $a \in \mathcal{A}(s)$. This Q-value estimates the expected future reward that the RL agent will receive after taking action a in state s ; the action with the highest Q-value is then the optimal action to take in that state. For large state and action spaces, a DNN can be trained to approximate the mapping from (s, a) to Q-value, as in DRL, where states and actions are described using feature sets.

B. DRL-based Forwarding Strategies

In principle, DRL can learn a forwarding strategy that is able to seamlessly adapt forwarding decisions to diverse network conditions by varying the feature values that are input into the associated neural network. This is unlike traditional adaptive forwarding approaches [31]–[33], which must first explicitly identify the current network setting and then switch to using the appropriate forwarding strategy for that setting. However, although it is relatively easy to train a DRL forwarding strategy in one network setting and obtain good testing performance in the same setting, training a strategy that performs effectively across diverse settings is more difficult given the time and resource-intensive nature of training.

A key objective of using DRL in this work is thus to ensure *generalizability* of the forwarding strategy, so that the strategy performs well across diverse network settings, including those on which it was not trained. To do so, we build on [9] in which DRL agents are defined for *packets*

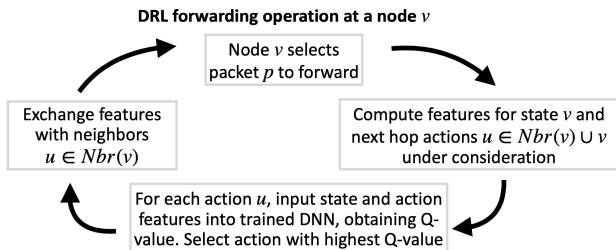


Fig. 1. Overview of DRL forwarding strategy of [9] on which we build.

rather than devices, and so packets themselves choose their next hops, simplifying learning. Features are then computed from a packet’s viewpoint and learning tracks packet states over time. Importantly, this forwarding strategy is able to be trained offline (so can be used directly in testing scenarios) and the same strategy can be used independently by all packets.

Fig. 1 illustrates the DRL formulation in [9]. Each node v in the network repeats the process of exchanging features with neighbors, selecting a packet p to forward, and having p choose a next hop action u . Packet p separately considers each possible action u available in its current state v by feeding the corresponding state and action features (see more in §III-D) into the DNN that encodes the forwarding strategy. The DNN then outputs a Q-value measuring the goodness of p moving from v to u , and the action with the highest Q-value is selected.

C. High-level Approach for Generalizability

Our approach for designing a DRL-based generalizable forwarding strategies has two parts: (i) *train a generalizable base model* and (ii) *fine-tune the base model when necessary*.

To train a generalizable base model, we leverage a combination of *novel features*, *continual learning (CL)*, and training on *diverse scenarios*. The performance of DRL-based forwarding depends heavily on the input features. We therefore design new features, beyond those in [9], to capture node diversity in network settings (see §IV). Training the model sequentially across multiple diverse scenarios can suffer from “catastrophic forgetting”, i.e., models trained on later scenarios do not perform well on earlier scenarios. We thus design CL-based forwarding strategies to achieve both plasticity and stability (see §V). Finally, we train the base model on a wide range of settings and large amount of data (80k timesteps for each setting), ensuring the model is exposed to adequate diversity. While CL allows the use of many training scenarios, we shall see that, with careful selection, only a few are needed to derive a generalizable base model.

In our evaluation, we find that it is often sufficient to use this base model directly in new scenarios. When necessary, we *fine-tune* this base model with a small amount of data from a new scenario. For instance, we use 1000 timesteps of data from a real road network in one city to fine-tune the base model, and then use it in 18 road network scenarios from two cities. This fine-tuning is one form of transfer learning [34]: it only uses a small number of samples since it applies the

knowledge gained from the diverse datasets contained in the base model.

D. Features for DRL-based Forwarding

Table I lists the features used in [9] and the new features (in bold) that we introduce and use in this work. Nodes exchange features only with their neighbors to limit the control overhead incurred by these exchanges. We briefly describe the features in [9] below; the new features are deferred to §IV.

Consider a packet p , with destination d , currently at device v with neighbors $Nbr(v)$. The *state features* for p are defined at multiple levels. Packet-level features capture information about p like p ’s time-to-live (TTL). Device-level features capture information about v like v ’s queue length, node degree and node density. Path-level features capture information about the time-varying path from v to d , like the number of packets at v with destination d , the estimated and possibly out-of-date Euclidean distance from v to d , and the transitive timer for v to d (computed as the time elapsed since v last met d , updated via timer transitivity [29]). Neighborhood-level features are then aggregate values (minimum, maximum, and mean) computed over the device and path-level features for $Nbr(v)$. The *action features* describe a possible next hop action $u \in Nbr(v) \cup v$ for packet p , i.e., moving to node u or staying at the current node v , and comprise the device-level and path-level features for u along with context features indicating whether p has recently visited u and whether the action type is to move to a neighbor or stay at the current node.

Although the above features were shown to be able to characterize a network’s conditions and generalize to different mobile network scenarios [9], they also have some critical limitations. First, they do not quantify the *quality or freshness of feature values*. When some features are of low quality or stale (e.g., not updated for a long time due to sparse network connectivity), the model might be better off ignoring them. Second, they fail to account for varying network conditions, such as nodes moving at different speeds or networks with both sparse and dense areas of connectivity. These limitations motivate the new features we introduce in §IV.

IV. NEW FEATURES FOR DIVERSE NETWORKS

To characterize diverse mobile wireless networks, we introduce three classes of features: *quality of information* metrics, *network memory* metrics, and *community* metrics. For each class, we propose specific features (shown in bold in Table I); exploring other possible features is left as future work. In the following, we describe these features and discuss their benefits. At the end of this section, we describe how we initialize and normalize feature values to ensure generalizability.

A. Quality of Information Metrics

In a mobile network, nodes may be able to only infrequently exchange features, decreasing the quality and timeliness of feature values. But without a way to measure feature quality, a node cannot distinguish whether its estimated value of a feature is close to or far from the true value of that feature. For

TABLE I

FEATURES FOR PACKET p AT TIME t WITH DESTINATION d LOCATED AT DEVICE v WITH POSSIBLE NEXT HOPS $u \in Nbr(v) \cup v$, WHERE x SPECIFIES THE VALUE OF A GIVEN FEATURE. THE FEATURES SHOWN IN BOLD ARE NEW IN THIS WORK (SEE §IV).

Level	Feature	Init. Val.	Raw Range	\bar{x}	Normalization
Packet	Time-to-live of packet p	-	$[0, T]$	-	$(x+1)/(T+1)$
Device	Queue length at v	-	$[0, B]$	-	$(x+1)/(B+1)$
	Node density of v	-	$[0, N-1]$	-	$\min(1, (x+1)/(N+1))$
	Node degree of v	-	$[0, N-1]$	-	$\min(1, (x+1)/(S+1))$
	Dynamic connectivity (short) , $\delta_s = 100s$	-	$[0, N-1]$	-	$(x+1)/N$
	Dynamic connectivity (long) , $\delta_l = 500s$	-	$[0, N-1]$	-	$(x+1)/N$
	Dispersion (short) , $\tau_s = 10s$	$L/20m$	$[0, L]$	-	$(x+1)/(L+1)$
	Dispersion (long) , $\tau_l = 100s$	$L/5m$	$[0, L]$	-	$(x+1)/(L+1)$
Path	Queue length at v for packets to d	$0.1B$	$[0, B]$	-	$(x+1)/(B+1)$
	Euclidean distance	$L/2m$	$[0, L]$	-	$(x+1)/(L+1)$
	Transitive timer	200s	$[0, \infty]$	200s	$1/(1+e^{-k(x-\bar{x})})$
	AoI	200s	$[0, \infty]$	200s	$1/(1+e^{-k(x-\bar{x})})$
Neighborhood	Aggregate (min, max, and mean) of device-level and path-level features of v 's neighbors	-	-	-	-
		-	-	-	-
Context	Boolean flags: relative visit history for p for action node u	-	-	-	-
	Boolean flags: transmit vs. stay	-	-	-	-

sparse networks, which have few opportunities to recover from bad forwarding decisions, feature values are also typically more out-of-date and uncertain than in dense networks, making it doubly critical to characterize quality. For example, in each setting in Table II, feature quality can be significantly worse for a transmission range of 20m compared to 80m.

Many metrics can be used to represent quality of information. In addition, different metrics may be appropriate for different features. For instance, for features estimating a distribution, such as inter-meeting time, variance could be used, while for other features, measures of confidence or freshness may be more appropriate. Here, we focus on feature freshness as a metric as it is relatively easy to measure, unlike, for instance, variance which can require many samples for accuracy and so is hard to estimate in sparse networks.

Age of information (AoI) [30]. We use AoI to characterize the freshness of features that are estimated using out-of-date information collected from other nodes. One such feature is Euclidean distance (see Table I). To estimate Euclidean distance, each node maintains the last known location of every other node w in the network along with a timer measuring the relative time Δ_w that has passed since that location was recorded; specifically, Δ_w starts at 0 and is incremented by one every timestep. When nodes meet, they exchange locations and timers for all nodes, update their own estimated locations to be those with the smallest timers, and increment each timer by one every timestep. The use of timers avoids the need for clock synchronization among devices. We then define AoI for those features associated with a node w simply as $AoI_w = \Delta_w$.

While AoI appears to be similar to the transitive timer feature in Table I [9], the main difference is that AoI directly measures the age of features (e.g., w 's location), while the transitive timer, introduced in utility-based forwarding (see [29]), is a heuristic to estimate the goodness of a node as a possible next hop. Specifically, the timer transitivity

calculation itself at a node v combines the age of w 's location information (as in AoI) with the time needed to travel the distance between node v and the neighboring node providing w 's location.

B. Network Memory Metrics

Intuitively, larger AoI values should indicate that the associated feature values are less accurate, but this is not necessarily always the case. Consider a mobile network in which nodes move in small loops. In this case, even if nodes move very fast, the estimated feature values may stay close to the true values for a long period of time. In contrast, for other kinds of node movement (such as that given by the random waypoint model), estimated feature values (like the Euclidean distance to a destination) may quickly diverge from their true values. More generally, some way to measure the rate of change in feature quality is needed. We call such measures *network memory metrics*: for instance, only in networks with short memory do large AoI values correlate with poor information quality.

Mixing time, which measures how quickly a node's location becomes independent from its current location, is a natural measure to quantify network memory. The study in [29] has characterized the asymptotic mixing time of RWP and random walk mobility, to gain insight into the impact of mixing time on the performance of different forwarding strategies. Yet, while the mixing time of RWP mobility can be estimated from average node speed and network area [28], estimating mixing time online for general node mobility requires a large number of samples and computationally expensive statistical calculation. Consequently, we explore other ways to quantify network memory.

Specifically, we quantify how quickly the quality of the estimated Euclidean distance feature decays as AoI increases, and use that as our network memory feature. We can relate the rate of decay of feature quality to the farthest distance

away that a node has moved from a previous location within a given time interval. For instance, if a node stays near the same location for a long time period, we expect that the quality of feature estimates for that node will remain consistent for a long period of time. Previous work [28] defines the locality of a mobility process to be the time scale over which the position of a node’s future location is correlated with its current location, and demonstrated empirically the locality of random walk and RWP mobility processes. This locality metric, however, is computationally intensive to estimate. We next propose a metric that we call *dispersion* that represents non-locality and can be estimated efficiently in an online distributed manner.

Dispersion. We define dispersion as the farthest Euclidean distance that a node travels away from a starting point during some time interval τ . When large distances are traveled by a node in a short period of time, then the node’s movements should have a short mixing time, and the quality of estimated features regarding the node should degrade quickly as its AoI increases. Consider a node v at location $(x_{t-\tau}, y_{t-\tau})$ at time $t - \tau$. Let $d_{t,\tau}$ be the maximum distance from $(x_{t-\tau}, y_{t-\tau})$ to any location that v is at during the interval $[t - \tau, t]$. We take an exponentially weighted average of $d_{t,\tau}$ over intervals to obtain the dispersion feature $D_\tau = \beta d_{t,\tau} + (1 - \beta)D_\tau^{prev}$ that we use, where $0 \leq \beta \leq 1$ and D_τ^{prev} is the previous estimate of dispersion. To quantify the rate of change of dispersion, we compute it for both a *short interval*, τ_s , and a *long interval*, τ_l . We consider the relatively short timescales of $\tau_s = 10s$ and $\tau_l = 100s$ (see Table I). in our evaluation in §VI.

C. Community Metrics

We refer to metrics that quantify the variety and rate of neighborhood changes as *community* metrics. In mobile networks, the neighborhood changes observed by nodes can be affected by many factors, including node speeds, movement patterns, and spatial distribution. The resulting changes in node neighborhoods can have a significant impact on forwarding decisions. For example, nodes that move faster than others will also meet other nodes more frequently, and hence might have a higher chance of quickly delivering a packet to its destination, and so could be favored as a packet’s next hop. However, in a densely connected network, even a node moving at a low speed might meet other devices fairly frequently, and hence, rather than forwarding its packets to fast nodes, a node could simply wait until it meets a packet’s destination. Doing so could avoid unnecessary forwards without increasing delay.

Dynamic connectivity. To quantify a node’s community, we extend the *dynamic connectivity* metric in [35], which quantifies the number of unique nodes encountered by a given node within a time interval, to consider two timescales (short and long) and design an online distributed approach for its estimation. The use of two timescales allows us to obtain the rate of change of dynamic connectivity. To compute dynamic connectivity, a node v first records the most recent time it met every other node in the network. Then at time t , node v counts the number of unique nodes that it saw within a short time interval $[t - \delta_s, t]$ and a long time interval $[t - \delta_l, t]$ to compute

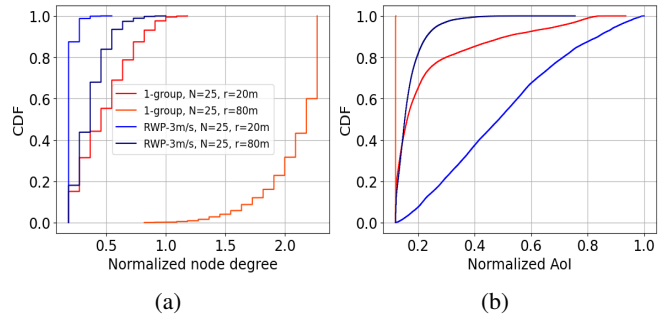


Fig. 2. Distributions of two feature across four network scenarios.

dynamic connectivity at two timescales. In our evaluation, we set $\delta_s = 100s$ and $\delta_l = 500s$ (see Table I).

D. Feature Initialization and Normalization

Our goal with feature initialization is to ensure that a feature always has a default value even when the information needed to estimate that feature is not available. This is specifically the case for time-averaged features (i.e., dispersion) and path features (which inherently describe a relationship between two nodes and so lack a value until those nodes meet or third-party information is shared). We initialize dispersion to $L = 1500m$, comparable to the size of the large networks that we evaluate. We initialize the path features to be close to the worst-case values we see in cumulative distribution functions (CDF) plots of feature values, to be conservative. For instance, we initialize destination queue length to a fraction of the maximum buffer size $B = 200$ in training (with $B = 2000$ in testing to ensure that no packets are dropped due to buffer overflow), and Euclidean distance to $L/2$. We initialize the temporal features of transitive timer and AoI to 200s, which approximates the time period for which features are expected to be good.

Our goal with normalization in Table I is to ensure that all features are relatively similar in terms of their scale of values to make DNN training easier. For features for which the maximum value is clear, that value can be directly used for normalization, such as time-to-live being bounded by the initial time-to-live of $T = 300$ in training (and $T = 3000$ in testing to avoid drops), rate of connectivity being bounded by the number of nodes in the network N , queue length being bounded by B , and dispersion being bounded by L . Node density we normalize by N , to capture the fraction of nodes in the network to which a node is connected, while node degree we normalize by a scaling factor of $S = 10$, to capture the point at which a network is unequivocally well-connected. For features that are unbounded, specifically the transitive timer and AoI, we use a shifted sigmoid function, $\sigma_k(x - \bar{x}) = \frac{1}{1 + \exp(-k(x - \bar{x}))}$ to force an upper bound on values. This is a non-linear mapping robust against outliers. The mean value, $\bar{x} = 200$, is set empirically, while $k = 0.01$ is a scaling factor varying how sharply values approach their upper limit.

V. CONTINUAL LEARNING BASED DRL FORWARDING

A. Methodology

Node diversity can give rise to drastically different kinds of network connectivity. For example, Fig. 2 shows the CDFs of two features. We see that the features differ significantly across the four network scenarios, sometimes with little overlap in distribution. CL addresses this by learning across a sequence of scenarios, retaining early knowledge from training, while incurring bounded computational resources and memory.

While many techniques have been proposed for CL, we focus on *experience replay* [36] coupled with *balanced reservoir sampling* [37]. This approach is simple and robust, and has been shown to be as effective as more sophisticated approaches [38]. The main idea of experience replay is to interleave past examples and current training examples. The approach of balanced reservoir sampling uses similar amounts of samples from each scenario so that the trained model is not biased toward any one scenario.

As in [9], [39], we use *centralized offline training* to train a DRL-based forwarding model; after training, each node uses the trained DRL model to make forwarding decisions independently in a *distributed online* manner. Offline training allows gathering of data from all nodes (which is not feasible in online training), leading to more effective training. To this end, we develop a network simulator to both generate training data and train the DRL model through CL.

For CL, we first train a DRL agent in the first scenario as in [9], [39], which do training in *rounds*. In each round, the current DRL model is used to make forwarding decisions, and the data collected so far is used for training at the end of the round. But unlike in [9], [39], after we complete training in the first scenario, we proceed to train in the second scenario, and so on. Consider training for round t in the k -th scenario, $k \geq 2$. Let $D_k(t)$ denote the data gathered so far in the k -th scenario. Let D_1, \dots, D_{k-1} denote the data gathered from the first $k-1$ scenarios. Each dataset is organized into state, action, reward, and next state tuples, (s, a, r, s') , where the corresponding state and action features include all of the features in Table I. To be computationally efficient, we use sampling, i.e., we take a fraction, α , of data from each dataset. For ease of exposition, assume $D_k(t)$ is the smallest dataset (since it is the current dataset being gathered, growing through round t and initially empty in the first round). Let $n = \max(\alpha|D_1|, \dots, \alpha|D_{k-1}|, \alpha|D_k(t)|)$. If $n \geq |D_k(t)|$, i.e., there is insufficient data in $D_k(t)$ even if all samples collected so far are included, we set n to $|D_k(t)|$. Then, we choose n samples uniformly randomly from each dataset, $D_1, \dots, D_k(t)$. The n samples in each dataset are divided into batches, each of size b . Finally, a batch is taken uniformly randomly from the k datasets until all batches have been used for training.

To summarize, the above approach uses the same amount of samples from each dataset, and mixes the batches from the k datasets uniformly randomly for training. In the rest of this paper, we use $\alpha = 10\%$ and $b = 32$. We also tried other

TABLE II

THE FULL SPACE OF POSSIBLE TRAINING SCENARIOS CONSIDERED FOR CL. THE THREE SETTINGS IN BOLD ARE THE ONLY ONES USED FOR CL.

Setting	\bar{v} (m/s)	Average node degree		
		$r = 20\text{m}$	$r = 50\text{m}$	$r = 80\text{m}$
RPGM 1-group	3.0	3.2	13.6	21.1
RPGM 2-group	3.0	1.8	7.2	11.1
RWP-3m/s	3.0	0.2	1.2	2.7
RWP-15m/s	15.0	0.2	1.0	2.5
RWP-mix1 (5,20)	12.6	0.2	1.0	2.5
RWP-mix2 (12,13)	9.2	0.2	1.1	2.7
RWP-mix3 (20,5)	5.4	0.2	1.1	2.7

*RPGM 2-group contains 24 nodes (12 nodes in each group), all others contain 25 nodes, moving in $500\text{ m} \times 500\text{ m}$ area. In mix settings, the #s of slow and fast nodes are marked (in order) in the parentheses.

options and found that using $\alpha = 5\%$ leads to worse results, while using $\alpha = 30\%$ leads to similar results as $\alpha = 10\%$; using $b = 64$ leads to similar results as $b = 32$.

B. Choosing Scenarios for Continual Learning

With the above CL algorithm, we can train a DRL agent using many scenarios sequentially. The more scenarios used, in principle, the more generalizable the trained model. However, training over many scenarios is time consuming and computationally intensive. Therefore, a guideline for CL is to carefully choose the training scenarios used to limit training time [12].

Space of possible training scenarios. We consider a total of $7 \times 3 = 21$ possible training scenarios as shown in Table II. These scenarios include Reference Point Group Mobility (RPGM) [40] with one or two groups, and Steady-state Random Waypoint (RWP) mobility [41], [42]. A node moves either *slow* (from 1 to 5m/s with mean of 3m/s) or *fast* (from 13 to 17m/s with mean of 15m/s). In RPGM 1-group and 2-group scenarios, all nodes are slow. For RWP mobility, we consider two homogeneous settings (all nodes are slow or fast) and three heterogeneous settings, RWP-mix1, RWP-mix2, and RWP-mix3, with the number of slow and fast nodes marked in Table II. The transmission range r varies from 20m to 80m, resulting in networks ranging from poorly- to well-connected. All mobility traces are generated using BonnMotion [43].

In each scenario, we generate time-varying traffic. Flows arrive following a Poisson distribution with parameter $.001N/25$, where N is the number of nodes in the network. Packets on a given flow arrive according to a Poisson distribution with parameter 0.01. Flow durations follow an exponential distribution with parameter 5000. We further assume sufficient bandwidth for all packets at a device to be transmitted in a single timestep.

Scenarios selected for CL. During CL, we start with the simplest mobility scenario, RPGM 1-group, with $r = 50\text{m}$. Then the second scenario selected is homogeneous RWP (specifically, RWP-3m/s, $r = 50\text{m}$), and the third scenario is heterogeneous RWP (specifically, RWP-mix2 which has a similar number of fast and slow nodes with $r = 20\text{m}$). These three scenarios, marked in bold in Table II, are for small networks (25 nodes in a $500\text{m} \times 500\text{m}$ area) so that training is

computationally efficient. As shown in Table II, they cover a wide range of settings, including three mobility settings, with the average node degree ranging from 0.2 to 13.6.

Although we only use three scenarios for CL, each scenario includes a large number of timesteps: 100K, with the last 40K timesteps as cool-down period¹, each timestep corresponding to one second. This allows us to fully capture the variability in each scenario. Note that for each scenario, training happens at the end of each round of 1K timesteps.

Training environment and parameters. We perform our simulations using a custom discrete-time packet-level simulator we wrote in Python3, and used version 2.13.1 of Keras [44] and Tensorflow [45]. The DNN has m feature inputs ($m = 63$, see Table I), two fully connected hidden layers (with $10m$ and $m/2$ nodes), and one output corresponding to the Q-value. We use the same reward function as in [9]: $r_{stay} = -1$ if the packet stays at its current node, $r_{transmit} = -2$ if the packet moves to a neighboring node, $r_{delivery} = 0$ if the packet reaches its destination, and $r_{drop} = r_{transmit}/(1 - \gamma)$ if the packet is dropped, corresponding to receiving $r_{transmit}$ for infinite time steps where $0 \leq \gamma \leq 1$ is the RL discount rate, and is set to 0.99. We use the ReLU activation function, Adam optimizer, mean squared error (MSE) loss, batch size of 32, 10 epochs, learning rate of 10^{-4} , and training validation split of 0.2. For the RL agent, we use an exploration rate, ϵ , of 0.1.

After completing CL, we verify that the model trained in the three scenarios is indeed generalizable to the 21 scenarios in Table II (figures omitted). Other testing results are detailed in §VI and §VII.

VI. EVALUATION IN LARGE NETWORKS

A. Evaluation Setup

We consider 36 test scenarios, each containing 100 nodes moving in a $1000\text{m} \times 1000\text{m}$ area. The first 21 scenarios are the same as those considered for training (Table II), except that they are $4 \times$ larger. The last $5 \times 3 = 15$ scenarios (5 speed configurations and 3 transmission ranges, consistent with RWP) are for Manhattan Grid mobility [43]. In this model, the area is divided into 20×20 grid blocks (each block of size $50\text{m} \times 50\text{m}$); nodes move along the grid lines, and can only change direction at the four corners of a block.

We compare our CL-trained DRL model, *DRL-CL*, with three other strategies. (i) *Oracle strategy*, which provides the best performance, but not achievable in practice due to the lack of oracle information. We obtain the results of this strategy through epidemic-based flooding [46], which leads to optimal delay when ignoring congestion. Specifically, we obtain the delivery delay for a packet as the delay when the first copy reaches the destination, and record the resource usage as the number of forwards of this copy. (ii) Two state-of-the-art heuristics, *Seek-and-focus* and *Utility-based* forwarding [29].

The performance metrics include *delivery rate*, *delivery delay*, and *number of forwards*. They quantify the percentage

¹No new packets are generated in cool-down period, so that all packets that have been generated are delivered by the end of the simulation.

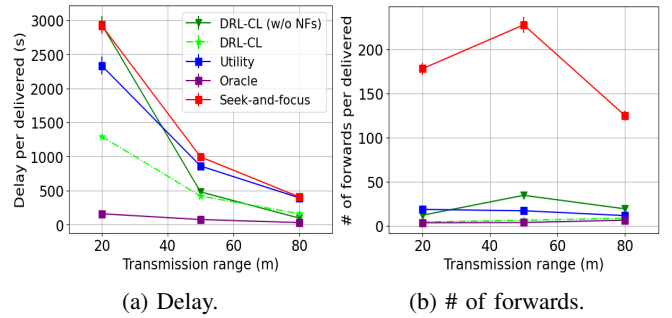


Fig. 3. Comparing DRL-CL with and without new features (NFs) and three other schemes, RWP-mix3 setting, large network.

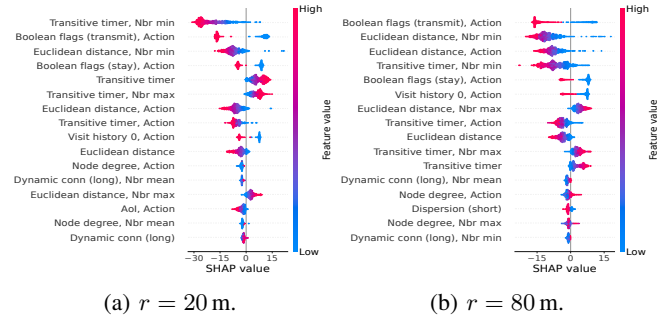


Fig. 4. Shapley values of the top-16 important features for DRL-CL, RWP-mix3 setting, large network.

of the packets delivered, and the delay and number of forwards for delivered packets. The latter two metrics present tradeoffs between performance and the amount of resources consumed.

B. Evaluation Results

We find that the new features (see §IV) are indeed helpful in capturing important network characteristics, leading to more generalizable models. As an example, we show the results for RWP-mix3 when the transmission range r varies from 20 to 80m. Fig. 3 shows the delay and number of forwards; all strategies lead to 100% delivery rate (omitted in figure). The model with new features significantly outperforms the one without new features: it leads to 57% lower delay when the $r = 20\text{m}$, and many fewer forwards overall. It also leads to 45% lower delay than the Utility-based scheme when $r = 20\text{m}$ and less forwards. Seek-and-focus leads to high delay and significantly more forwards than do the other schemes. Fig. 4 shows the top-16 important features obtained by SHAP [47] when the transmission range is 20 or 80m. We see that which features are important differ across the scenarios; for both, we see our proposed new features (AoI, dispersion, and dynamic connectivity) among the top-16 features.

We further find that the CL-trained model on three scenarios (see §V-B) leads to a more generalizable model than models trained only in one or two scenarios. Fig. 5 compares the results of DRL-CL with those of ‘model-1’ and ‘model-2’ (i.e., the models at the end of the first or second scenario in CL). DRL-CL significantly outperforms the other two models when the transmission range is 20 or 50m. This is perhaps not surprising since the third scenario used in DRL-CL is for a

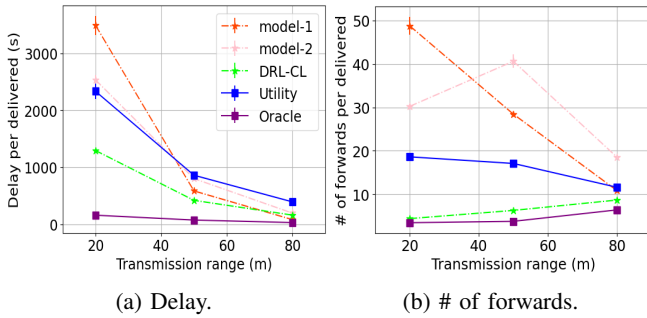


Fig. 5. Comparing DRL-CL with models after training in first two scenarios (marked as ‘model-1’ and ‘model-2’), RWP-mix3 setting, large network.

transmission range of 20m with mixed speed. We confirm that DRL-CL performs better for other scenarios (figures omitted).

Overall results. Table III lists the delay and number of forwards for all 36 test scenarios. The three results listed in each cell are the average results for Oracle, DRL-CL, and Utility-based forwarding, respectively; the results for Seek-and-focus are omitted since it generally performs worse than Utility-based forwarding. For each setting, we run 5 simulations (each includes 50K timesteps, with the last 20K as the cool-down period) and confirm that the 95% confidence intervals are tight. We only show the average delay and number of forwards since the delivery rate is 100% for all strategies, except for one case (Grid-3m/s, $r = 20$ m), where DRL-CL and Utility-based forwarding have delivery rate of 96% and 95%, respectively.

As expected, we see from Table III that DRL-CL performs worse than the Oracle scheme for all cases. Conversely, DRL-CL generally outperforms Utility-based forwarding. It only exhibits higher delay in one case (1-group mobility, $r = 80$ m). However, in this case, both delay values are relatively low (61s for DRL-CL vs. 33s for Utility-based forwarding). For two homogeneous slow-node settings, RWP-3m/s and Grid-3m/s, with $r = 20$ m (sparse connectivity), DRL-CL leads to significantly more forwards than Utility-based forwarding. The base model does not perform well for these two cases since the only sparse setting that it is trained on has mixed speed, instead of homogeneous speed. We therefore fine-tune the base model using 2000s of data from RWP-3m/s, $r = 20$ m. Specifically, we take the base model as the initial model and then the 2000s of data to fine-tune the model in rounds (each round is set to 50s). We see that the fine-tuned model leads to similar delay as the base model, while significantly fewer forwards (see bold results for these two cases in Table III). Using this fine-tuned model for these two mobility settings with $r = 50$ m also reduces the number of forwards, but it is less effective in highly connected scenarios (when $r = 80$ m).

To summarize, our approach is generalizable to the 36 scenarios Table III: it achieves lower delay than Utility-based forwarding, with reduction up to 78% (specifically, 194s vs. 873s in RWP-3m/s, $r = 80$ m), except for one case where both schemes have low delay. In addition, with fine-tuning using only 2000s of data in one case, it leads to comparable or slightly more forwards than Utility-based forwarding.

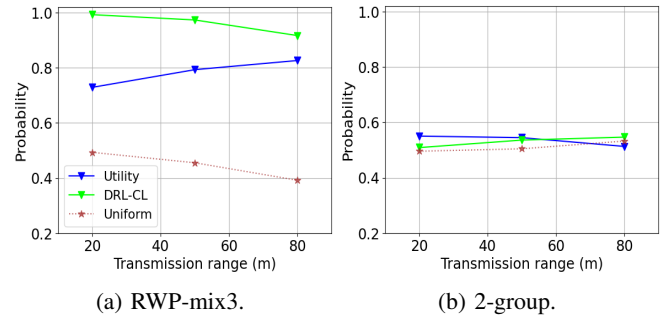


Fig. 6. Forwarding preferences of different forwarding policies.

Forwarding behavior. In mixed-speed scenarios with sparse connectivity, intuitively, it is generally better to forward packets to faster nodes, as they can cover greater distances more quickly, enabling faster delivery to the destination. We examine whether DRL-CL has this behavior. Specifically, for all decision makings when a node’s neighbors contain both fast and slow nodes, we obtain the probability that DRL-CL chooses a fast node. For comparison, we also obtain the corresponding probability for Utility-based forwarding and when following a uniform random policy. We find that DRL-CL indeed prefers fast nodes. Fig. 6a shows an example for RWP-mix3. We see DRL-CL has higher probability of choosing fast nodes than Utility-based strategy and uniform choice, and the probability decreases with the transmission range, while Utility-based strategy shows the opposite trend. Similarly, for 2-group scenarios, we examine whether DRL-CL prefers forwarding to a neighbor that is in the same group as the destination. Fig. 6b shows that DRL-CL has slightly higher probability of choosing a neighbor in the destination group than the uniform choice.

VII. HANDLING REAL-WORLD SCENARIOS

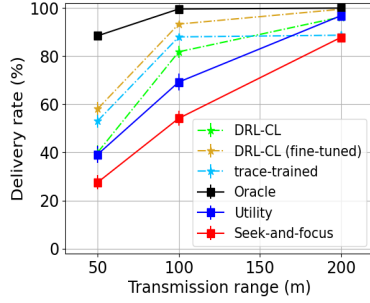
We now evaluate DRL-CL in real-world scenarios, where nodes (e.g., pedestrians and vehicles) navigate along urban road networks. For this purpose, we use Simulation of Urban MObility (SUMO) [48], which inputs realistic information (e.g., road networks, infrastructure, traffic lights) to simulate urban traffic based on transportation science. We consider road networks in two cities, one for Bologna, Italy [49] and the other for Bad Hersfeld, Germany [50].

The road network for Bologna spans an area of roughly $1500\text{m} \times 1500\text{m}$. Since a node can move out of the network, we choose intervals of 1000 seconds and only consider the nodes that remain in the network throughout the interval. By varying the time intervals, we obtained three scenarios (BO-1, BO-2, BO-3), with the three highest number of nodes ($N = 135$ to $N = 238$ nodes). The road network for Bad Hersfeld spans a much larger area. We select areas of size $1500\text{m} \times 1500\text{m}$ and vary the time to select three scenarios (BA-1, BA-2, BA-3) with the most nodes ($N = 44$ to $N = 53$ nodes). The transmission range is set to 50 to 200m, leading to $3 \times 3 = 9$ scenarios for each city, with average node degree 5.4 to 35.4 for Bologna, and from 1.8 to 10.2 for Bad Hersfeld. For each

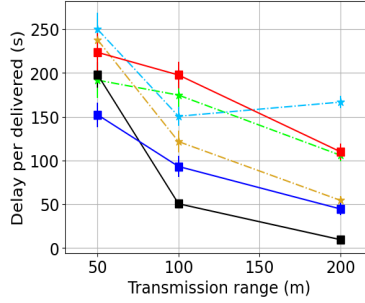
TABLE III

LARGE-SCALE (100 NODES IN 1000 M \times 1000 M AREA) TESTING RESULTS. EACH CELL LISTS RESULTS IN THE ORDER OF ORACLE, DRL-CL, UTILITY-BASED FORWARDING. IN TWO ROWS, RESULTS IN BOLD ARE FROM THE FINE-TUNED MODEL USING RWP-3M/S, $r = 20$ M.

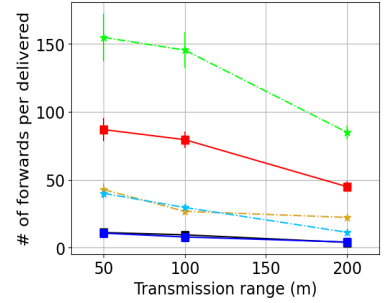
Setting	Delay (s)			# of forwards		
	$r = 20$ m	$r = 50$ m	$r = 80$ m	$r = 20$ m	$r = 50$ m	$r = 80$ m
1-group	113, 690, 1522	18, 63, 175	5, 61, 33	4, 67, 22	5, 22, 8	3, 40, 4
2-group	124, 942, 1594	24, 67, 254	6, 38, 52	4, 56, 21	6, 25, 9	4, 22, 4
RWP-3m/s	342, 5138 (4853), 5542	167, 1324 (1113), 2261	51, 194, 873	3, 120 (10), 27	4, 59 (31), 26	8, 35, 17
RWP-15m/s	66, 1029, 1076	36, 332, 396	18, 142, 222	3, 5, 15	3, 4, 12	6, 5, 9
RWP-mix1 (20,80)	74, 1094, 1169	39, 352, 506	19, 148, 322	3, 5, 16	3, 4, 15	6, 5, 12
RWP-mix2 (50,50)	98, 1189, 1455	49, 380, 640	22, 159, 390	4, 5, 16	4, 4, 16	6, 6, 13
RWP-mix3 (80,20)	159, 1293, 2332	74, 419, 860	30, 160, 393	3, 4, 19	4, 6, 17	6, 9, 12
Grid-3m/s	628, 7817 (7999), 8155	427, 3706 (4492), 6342	158, 561, 1924	4, 584 (7), 27	4, 688 (17), 41	7, 71, 27
Grid-15m/s	124, 1779, 1779	84, 984, 1073	40, 374, 564	4, 11, 17	4, 11, 19	6, 13, 15
Grid-mix1 (20,80)	135, 1884, 1975	92, 1060, 1278	44, 424, 625	4, 10, 18	4, 10, 21	6, 12, 16
Grid-mix2 (50,50)	171, 2038, 2494	117, 1177, 1575	53, 502, 714	4, 9, 19	4, 9, 22	6, 11, 16
Grid-mix3 (80,20)	267, 2203, 3581	182, 1306, 2081	79, 571, 887	4, 10, 20	4, 12, 22	6, 12, 17



(a) Delivery rate.



(b) Delay.



(c) # of forwards.

Fig. 7. Results for a real-world scenario in Bologna (BO-1).

TABLE IV

RESULTS FOR REAL-WORLD SCENARIOS IN BOLOGNA (BO) AND BAD HERSFELT (BA). NODES MOVE IN 1500M \times 1500M AREAS. EACH CELL LISTS THE RESULTS IN THE ORDER OF ORACLE, DRL-CL (FINE-TUNED), AND UTILITY. THE FINE-TUNING USES A SINGLE SCENARIO, BO-1, $r = 100$ M.

Setting	N	Delivery rate (%)			Delay (s)			# of forwards		
		$r = 50$ m	$r = 100$ m	$r = 200$ m	$r = 50$ m	$r = 100$ m	$r = 200$ m	$r = 50$ m	$r = 100$ m	$r = 200$ m
BO-1	238	88, 58, 39	100, 93, 69	100, 99, 97	198, 238, 152	51, 122, 93	10, 54, 45	11, 43, 11	10, 27, 8	4, 22, 4
BO-2	213	87, 51, 41	100, 90, 76	100, 99, 99	212, 160, 140	68, 156, 129	6, 69, 41	10, 30, 11	9, 26, 9	4, 27, 4
BO-3	135	94, 66, 52	100, 97, 93	100, 100, 100	158, 212, 174	42, 70, 71	9, 41, 14	10, 39, 11	7, 14, 7	3, 17, 3
BA-1	53	60, 40, 39	86, 77, 67	100, 96, 91	177, 160, 153	114, 117, 100	47, 59, 48	4, 15, 5	4, 10, 4	3, 5, 3
BA-2	49	59, 33, 35	74, 60, 54	100, 94, 90	228, 167, 184	155, 149, 148	72, 88, 78	3, 13, 3	4, 14, 4	3, 12, 3
BA-3	44	59, 42, 34	73, 64, 59	97, 92, 89	198, 172, 164	111, 92, 87	49, 55, 54	3, 14, 4	4, 7, 5	3, 8, 3

scenario, we generate packets among nodes using a similar process as in §V-B.

Fine-tuning base model. We find that the base model does not perform well in the above scenarios. This is perhaps not surprising since it is trained using synthetic mobility models, which differs significantly from real-world mobility in road networks. We therefore fine-tune the base model using one trace of duration 1000s for Bologna (BO-1), $r = 100$ m. Specifically, we take the base model as the initial model and fine-tune it using 1000s of packet trace from BO-1.

Testing results. We test this fine-tuned model in the 18 scenarios across the two cities. For each scenario, we generate 30 packet traces and obtain the average results with 95% confidence intervals. The duration of each trace is 1000s (the last 300s is the cool-down period). We next detail the results for BO-1, and then the results for all scenarios.

Fig. 7 shows the result for BO-1. The delivery rate is below 100% for all the schemes due to the short interval (1000s). DRL-CL (fine-tuned) outperforms DRL-CL (i.e., without fine-tuning), and leads to much higher delivery rate than Utility-based forwarding, which further outperforms Seek-and-focus (we omit the results for Seek-and-focus in the following due to its generally worse performance). Since DRL-CL (fine-tuned) achieves higher delivery rates than Utility-based forwarding, it is reasonable that DRL-CL (fine-tuned) leads to higher delays and more forwards—in fact, sometimes Oracle scheme has higher delays than Utility-based forwarding as well. We further train a DRL model directly using the data that was used for fine-tuning the base model. The test results for this model are marked as ‘trace-trained’ in Fig. 7. We see that it does not generalize well: it leads to much lower delivery rate when $r = 200$ m (even lower than that when $r = 100$ m) than other

schemes. This is perhaps not surprising since it is trained only using a small amount (1000s) of data. In contrast, this small amount of data is sufficient for our fine-tuning since it builds on the knowledge embedded in the base model.

Table IV lists the results using the above fine-tuned model for all the 18 scenarios across the two cities. It achieves up to 24% (specifically, 93% vs. 69% for BO-1, $r = 100\text{m}$) higher delivery rate than Utility-based forwarding. In the cases where these two schemes have similar delivery rate (BO-1, BO-2, BO-3, when $r = 200\text{m}$), the fine-tuned model has slightly higher delay and more forwards. Overall, our approach generalizes well to the 18 real-world scenarios.

VIII. CONCLUSIONS

In this paper, we have developed a framework for training generalizable DRL-based forwarding strategies for mobile wireless networks. We proposed three new classes of features for characterizing diverse networks and a CL-based approach for adapting forwarding to diverse networks. Extensive evaluation in a wide range of scenarios, including real-world road networks, demonstrates that our approach leads to generalizable forwarding strategies.

REFERENCES

- [1] D. B. Johnson and D. A. Maltz, "Dynamic source routing in ad hoc wireless networks," in *Mobile Computing*. Alphen aan den Rijn, Netherlands: Kluwer Academic Publishers, 1996, pp. 153–181.
- [2] C. Perkins, E. Belding-Royer, and S. Das, "Rfc3561: Ad hoc on-demand distance vector (AODV) routing," 2003.
- [3] T. Clausen, P. Jacquet, C. Adjih, A. Laouiti, P. Minet, P. Muhlethaler, A. Qayyum, and L. Viennot, "Rfc 3626 optimized link state routing protocol (OLSR)," 2003.
- [4] C. E. Perkins and P. Bhagwat, "Highly dynamic destination-sequenced distance-vector routing for mobile computers," in *SIGCOMM*, 1994.
- [5] S. Jain, K. Fall, and R. Patra, "Routing in a delay tolerant network," in *Proc. of SIGCOMM*, 2004.
- [6] V. Manfredi, M. Crovella, and J. Kurose, "Understanding stateful vs stateless communication strategies for ad hoc networks," in *Proc. of Mobicom*, 2011, pp. 313–324.
- [7] R. S. Sutton and A. G. Barto, *Reinforcement learning: An introduction*. Cambridge, MA: MIT press, 2018.
- [8] Y. Bengio, "Learning deep architectures for AI," *Foundations and trends® in Machine Learning*, vol. 2, no. 1, pp. 1–127, 2009.
- [9] V. Manfredi, A. P. Wolfe, X. Zhang, and B. Wang, "Learning an adaptive forwarding strategy for mobile wireless networks: resource usage vs. latency," *Machine Learning*, vol. 113, no. 10, pp. 7157–7193, 2024.
- [10] M. D. Lange, R. Aljundi, M. Masana, S. Parisot, X. Jia, A. Leonardis, G. G. Slabaugh, and T. Tuytelaars, "A continual learning survey: Defying forgetting in classification tasks," *IEEE Trans. Pattern Anal. Mach. Intell.*, vol. 44, no. 7, pp. 3366–3385, 2022.
- [11] K. Kheterpal, M. Riemer, I. Rish, and D. Precup, "Towards continual reinforcement learning: A review and perspectives," *J. Artif. Intell. Res.*, vol. 75, pp. 1401–1476, 2022.
- [12] L. Wang, X. Zhang, H. Su, and J. Zhu, "A comprehensive survey of continual learning: Theory, method and application," *IEEE Trans. Pattern Anal. Mach. Intell.*, vol. 46, no. 8, pp. 5362–5383, 2024.
- [13] J. A. Boyan and M. L. Littman, "Packet routing in dynamically changing networks: A reinforcement learning approach," in *NIPS*, 1994.
- [14] H. A. Al-Rawi, M. A. Ng, and K.-L. A. Yau, "Application of reinforcement learning to routing in distributed wireless networks: a review," *Artificial Intelligence Review*, vol. 43, no. 3, pp. 381–416, 2015.
- [15] Z. Mammeri, "Reinforcement learning based routing in networks: Review and classification of approaches," *IEEE Access*, 2019.
- [16] N. C. Luong, D. T. Hoang, S. Gong, D. Niyato, P. Wang, Y.-C. Liang, and D. I. Kim, "Applications of deep reinforcement learning in communications and networking: A survey," *IEEE Communications Surveys & Tutorials*, vol. 21, no. 4, pp. 3133–3174, 2019, fourth Quarter.
- [17] Q. Mao, F. Hu, and Q. Hao, "Deep learning for intelligent wireless networks: A comprehensive survey," *IEEE Communications Surveys & Tutorials*, vol. 20, no. 4, pp. 2595–2621, 2018, fourth Quarter.
- [18] F. Li, X. Song, H. Chen, X. Li, and Y. Wang, "Hierarchical routing for vehicular ad hoc networks via reinforcement learning," *IEEE Transactions on Vehicular Technology*, vol. 68, no. 2, pp. 1852–1865, 2018.
- [19] A. Lolai, X. Wang, A. Hawbani, F. A. Dharejo, T. Qureshi, M. U. Farooq, M. Mujahid, and A. H. Babar, "Reinforcement learning based on routing with infrastructure nodes for data dissemination in vehicular networks (RRIN)," *Wireless Networks*, pp. 1–16, 2022.
- [20] L. Luo, L. Sheng, H. Yu, and G. Sun, "Intersection-based v2x routing via reinforcement learning in vehicular ad hoc networks," *IEEE Transactions on Intelligent Transportation Systems*, 2021.
- [21] M. Feng, L. Qian, and H. Xu, "Multi-robot enhanced MANET intelligent routing at uncertain and vulnerable tactical edge," in *MILCOM*, 2018.
- [22] B. Sliwa, C. Schüler, M. Patchou, and C. Wietfeld, "Parrot: Predictive ad-hoc routing fueled by reinforcement learning and trajectory knowledge," in *IEEE Vehicular Technology Conference*, 2021.
- [23] A. Rovira-Sugranes, F. Afghah, J. Qu, and A. Razi, "Fully-echoed q-routing with simulated annealing inference for flying adhoc networks," *IEEE Trans. on Network Science and Engineering*, vol. 8, no. 3, 2021.
- [24] X. Qiu, L. Xu, P. Wang, Y. Yang, and Z. Liao, "A data-driven packet routing algorithm for an unmanned aerial vehicle swarm: A multi-agent reinforcement learning approach," *IEEE Wireless Communications Letters*, vol. 11, no. 10, pp. 2160–2164, 2022.
- [25] D. K. Sharma, J. J. Rodrigues, V. Vashishth, A. Khanna, and A. Chhabra, "RLProph: a dynamic programming based reinforcement learning approach for optimal routing in opportunistic IoT networks," *Wireless Networks*, vol. 26, no. 6, pp. 4319–4338, 2020.
- [26] F. Lozano-Cuadra, B. Soret, I. Leyva-Mayorga, and P. Popovski, "Continual deep reinforcement learning for decentralized satellite routing," *IEEE Trans. Commun.*, 2025.
- [27] H. Sun, W. Pu, X. Fu *et al.*, "Learning to continuously optimize wireless resource in a dynamic environment: A bilevel optimization perspective," *IEEE Trans. Signal Process.*, vol. 70, pp. 1900–1917, 2022.
- [28] H. Dubois-Ferriere, M. Grossglauser, and M. Vetterli, "Age matters: Efficient route discovery in mobile ad hoc networks using encounter ages," in *ACM MobiHoc*, 2003.
- [29] T. Spyropoulos, K. Psounis, and C. S. Raghavendra, "Single-copy routing in intermittently connected mobile networks," in *SECON*, 2004.
- [30] R. D. Yates, Y. Sun, D. R. Brown, S. K. Kaul, E. Modiano, and S. Ulukus, "Age of information: An introduction and survey," *IEEE JSAC*, vol. 39, no. 5, pp. 1183–1210, 2021.
- [31] C. Danilov, T. R. Henderson, T. Goff, O. Brewer, J. H. Kim, J. Macker, and B. Adamson, "Adaptive routing for tactical communications," in *IEEE Military Communications Conference*, 2012.
- [32] A. Seetharam, S. Heimlicher, J. Kurose, and W. Wei, "Routing with adaptive flooding in heterogeneous mobile networks," in *Proc. of COM-SNETS*, 2015.
- [33] M. Asadpour, K. A. Hummel, D. Giustiniano, and S. Draskovic, "Route or carry: Motion-driven packet forwarding in micro aerial vehicle networks," *IEEE Trans. on Mobile Computing*, vol. 16, no. 3, 2016.
- [34] S. J. Pan and Q. Yang, "A survey on transfer learning," *IEEE Trans. Knowl. Data Eng.*, vol. 22, no. 10, pp. 1345–1359, Oct 2010.
- [35] T. Spyropoulos, K. Psounis, and C. S. Raghavendra, "Efficient routing in intermittently connected mobile networks: The multiple-copy case," *IEEE/ACM Transactions on Networking*, vol. 16, no. 1, pp. 77–90, 2008.
- [36] R. Ratcliff, "Connectionist models of recognition memory: constraints imposed by learning and forgetting functions," *Psychological review*, 1990.
- [37] J. S. Vitter, "Random sampling with a reservoir," *ACM Transactions on Mathematical Software (TOMS)*, vol. 11, no. 1, pp. 37–57, 1985.
- [38] P. Buzzega, M. Boschini, A. Porrello, and S. Calderara, "Rethinking experience replay: a bag of tricks for continual learning," in *ICPR*, 2020.
- [39] V. Manfredi, A. P. Wolfe, X. Zhang, and B. Wang, "Learning an adaptive forwarding strategy for mobile wireless networks: Resource usage vs. latency," in *RLRealLife Workshop in NeurIPS*, 2022.
- [40] X. Hong, M. Gerla, G. Pei, and C.-C. Chiang, "A group mobility model for ad hoc wireless networks," in *MSWiM*, 1999.
- [41] W. Navidi and T. Camp, "Stationary distributions for the random waypoint mobility model," *IEEE Transactions on Mobile Computing*, vol. 3, no. 1, pp. 99–108, 2004.
- [42] J.-Y. Le Boudec and M. Vojnovic, "Perfect simulation and stationarity of a class of mobility models," in *IEEE Infocom*, 2005.

- [43] N. Aschenbruck, R. Ernst, E. Gerhards-Padilla, and M. Schwaborn, "Bonnmotion: a mobility scenario generation and analysis tool," in *International ICST conference on simulation tools and techniques*, 2010.
- [44] F. Chollet *et al.* (2015) Keras. [Online]. Available: <https://github.com/fchollet/keras>
- [45] M. Abadi and et al, "TensorFlow: Large-scale machine learning on heterogeneous systems," 2015. [Online]. Available: <http://tensorflow.org/>
- [46] A. Vahdat and D. Becker, "Epidemic routing for partially connected ad hoc networks," Duke Univ., Tech. Rep., 2000.
- [47] S. M. Lundberg and S.-I. Lee, "A unified approach to interpreting model predictions," in *NIPS*, 2017.
- [48] M. Behrisch, L. Bieker-Walz, J. Erdmann, and D. Krajzewicz, "SUMO – simulation of urban mobility: An overview," in *Proc. of SIMUL*, 2011.
- [49] L. Bieker, D. Krajzewicz, A. P. Morra, C. Michelacci, and F. Cartolano, "Traffic simulation for all: A real world traffic scenario from the city of bologna," in *Proc. of the SUMO Conference*. Springer, 2014.
- [50] F. Gotzler, F. Neumann, and L. Adenaw, "Assessment of personal rapid transit system configurations regarding efficiency and service quality," *Future Transportation*, vol. 2, no. 3, pp. 734–752, 2022.